Temperature dependent polarization reversal mechanism in 0.94(Bi1/2Na1/2) TiO3-0.06Ba(Zr0.02Ti0.98)O3 relaxor ceramics

Glaum, Julia; Simons, Hugh; Hudspeth, Jessica; Acosta, Matias; Daniels, John E.

Published in:
Applied Physics Letters

Link to article, DOI:
10.1063/1.4937586

Publication date:
2015

Document Version
Publisher's PDF, also known as Version of record

AIP | Applied Physics Letters

Temperature dependent polarization reversal mechanism in 0.94(Bi1/2Na1/2)TiO3-0.06Ba(Zr0.02Ti0.98)O3 relaxor ceramics

Julia Glaum, Hugh Simons, Jessica Hudspeth, Matias Acosta, and John E. Daniels

Citation: Applied Physics Letters **107**, 232906 (2015); doi: 10.1063/1.4937586
View online: http://dx.doi.org/10.1063/1.4937586
View Table of Contents: http://scitation.aip.org/content/aip/journal/apl/107/23?ver=pdfcov
Published by the AIP Publishing

Temperature dependent polarization reversal mechanism in $0.94(Bi_{1/2}Na_{1/2})TiO_3$-$0.06Ba(Zr_{0.02}Ti_{0.98})O_3$ relaxor ceramics

Julia Glaum,[1,a)] Hugh Simons,[2] Jessica Hudspeth,[3] Matias Acosta,[4] and John E. Daniels[1]
[1]*School of Materials Science and Engineering, UNSW Australia, Sydney, New South Wales 2052, Australia*
[2]*Department of Physics, Technical University of Denmark, 2800 Kgs. Lyngby, Denmark*
[3]*Structure of Materials Group, European Synchrotron Radiation Facility, 38043 Grenoble, France*
[4]*Institute of Materials Science, Technische Universität Darmstadt, 64287 Darmstadt, Hesse, Germany*

(Received 16 September 2015; accepted 30 November 2015; published online 10 December 2015)

The temperature at which the electric field induced long-range ordered ferroelectric state undergoes transition into the short-range ordered relaxor state, T_{F-R}, is commonly defined by the onset of strong dispersion of the dielectric permittivity. However, this combined macroscopic property and structural investigation of the polarization reversal process in the prototypical lead-free relaxor $0.94(Bi_{1/2}Na_{1/2})TiO_3$-$0.06Ba(Zr_{0.02}Ti_{0.98})O_3$ reveals that an applied electric field can trigger depolarization and onset of relaxor-like behavior well below T_{F-R}. The polarization reversal process can as such be described as a combination of (1) ferroelectric domain switching and (2) a reversible phase transition between two polar ferroelectric states mediated by a non-polar relaxor state. Furthermore, the threshold fields of the second, mediated polarization reversal mechanism depend strongly on temperature. These results are concomitant with a continuous ferroelectric to relaxor transition occurring over a broad temperature range, during which mixed behavior is observed. The nature of polarization reversal can be illustrated in electric-field-temperature (E-T) diagrams showing the electric field amplitudes associated with different polarization reversal processes. Such diagrams are useful tools for identifying the best operational temperature regimes for a given composition in actuator applications. © *2015 AIP Publishing LLC*.
[http://dx.doi.org/10.1063/1.4937586]

The piezoelectric system $(1-x)(Bi_{1/2}Na_{1/2})TiO_3$-$xBaTiO_3$ (BNT-BT) is an appealing replacement for lead-based materials in actuator applications due to its typically large piezoelectric coefficient, d_{33}, and normalized strain S_{max}/E_{max}.[1] Its strong electromechanical response is suggested to originate from the lone pair $6s^2$ electron system provided by the Bi-based component.[2] Many BNT-BT-based compositions are characteristically similar to well-known relaxor materials such as lead-lanthanum-zirconate-titanate (PLZT) or lead-magnesium-niobate (PMN).[3,4] This includes dispersive behavior of the temperature dependent permittivity and the possibility for a sufficiently large electric field to induce a polar phase in the macroscopically non-polar material.[5,6] These relaxor characteristics are determined by the disorder of the A- and B-site sublattices, and as such are sensitive to variations in composition[7–9] and temperature.[10]

Cooling from the high-temperature, paraelectric state leads to localized symmetry-breaking (i.e. short-range order) at the Burns temperature T_B and the formation of polar nano-regions in the overall non-polar matrix that are subject to strong thermal fluctuations (ergodic state).[11] With further cooling, a glass-like transition occurs at the freezing temperature T_f where the thermal fluctuations of the polar nano-regions vanish (non-ergodic state).[4] For the system under discussion, the nature of these polar regions has been described as antiferroelectric[12] or weakly polar ferrielectric.[13] Due to the insufficient correlation length, the polar regions act as independent entities giving rise to strong frequency dispersion of the dielectric properties.[14] The application of a sufficiently large electric field to a sample in the non-ergodic state can induce an irreversible transformation of the whole sample volume into a polar state exhibiting ferroelectric characteristics.[15] Critically, this electrically induced ferroelectric state can decay into the relaxor state upon heating. The temperature T_{F-R} marks this thermal transformation from long-range to short-range order, generally defined as the transition between the non-dispersive and dispersive region of the temperature dependent permittivity.[16] The highest unipolar polarizations and strains were found to be achieved close to this temperature.[17] However, measurements of the thermally stimulated depolarization currents (TSDC) provide a depolarization temperature T_d that is slightly lower than T_{F-R},[18] indicating that ferroelectric domains are spatially randomized before the loss of correlation occurs.[19]

Previous work on Zr-modified 0.94BNT-0.06BT ceramics, however, revealed that ferroelectric properties begin to degenerate at even lower temperatures than the nominal T_{F-R} or T_d,[9] suggesting that the temperature dependent decay from the ferroelectric to the relaxor state occurs over a broad temperature range rather than at a distinct temperature. Given the significant large-signal polarization and strain response associated with the electric-field induced relaxor to ferroelectric transition,[20] the continuous nature of the temperature dependent decay could significantly impact the applicability of these materials in piezoelectric devices.

This study therefore aims to determine how the mechanisms of electrical poling and polarization reversal depend

a)Author to whom correspondence should be addressed. Electronic mail: julia.glaum@ntnu.no

on the temperature-dependent ferroelectric to relaxor transition. We use a combination of large-signal macroscopic measurements and *in-situ* synchrotron x-ray diffraction to correlate the electric-field-dependent switching and depolarization currents to the changes of the average crystal structure during electric field induced polarization reversal as a function of temperature.

Disk shaped ceramic samples of composition $0.94(Bi_{1/2}Na_{1/2})TiO_3$-$0.06Ba(Zr_{0.02}Ti_{0.98})O_3$ were prepared by conventional solid-state processing.[21] The disks were polished to 1200 grit and annealed at 400 °C for 2 h to minimize internal stresses. Electrodes of silver paste (RS Components, Smithfield, Australia) were applied and dried at 50 °C.

Temperature dependent polarization, corresponding current density, and mechanical strain were measured using an aixACCT TFAnalyzer2000 system equipped with a Trek 20/20 high voltage amplifier, a SIOS laser interferometer (SP-S 120/500), and a Eurotherm 2416 PID temperature controller. The measurements were conducted at $f = 0.1$ Hz using a triangular, bipolar signal at a maximum electric field of $E = 4$ kV/mm. The measured sample used for macroscopic electromechanical measurements was depolarized at 350 °C for 5 min between measurements. To capture the broad temperature range, where the non-ergodic to ergodic transition occurs, measurements were taken from room temperature up to 100 °C ($T_{F\text{-}R} = 87$ °C for this composition).

The temperature dependent permittivity of an electrically poled sample was measured upon heating with 2 K/min from room temperature to 450 °C (Fig. 1(d)) using an Agilent HP4284A impedance analyzer. The excitation voltage was 1 V. It is from this data that the transition temperature $T_{F\text{-}R}$ of the given composition was extracted.

High-energy synchrotron XRD was carried out at beamline ID15B of the European Synchrotron Radiation Facility. A beam energy of 87.02 keV was used in conjunction with a large area detector (Pixium 4700)[22] to collect the full diffraction rings. Samples of the same processing batch and dimensions as used for the electromechanical measurements were placed in a specifically designed electric field cell.[23] Bipolar triangular electric field waveforms of frequency 0.1 Hz and electric field amplitude of ~4.5 kV/mm were applied to the samples at various temperatures, while XRD patterns were collected at a frequency of 2 Hz. The data were radially integrated into 10° azimuthal sections. Further details of the analysis of electric-field-induced strain using this setup are provided by Daniels *et al.*[23,24]

Figure 1(a) depicts the temperature dependent bipolar polarization loops measured upon initial electric field application from the unpoled state. At room temperature, saturated loops with a maximum polarization P_{max} of ~40 μC/cm^2 and a coercive field E_c of ~2.7 kV/mm are achieved. While P_{max} reduces only slightly at elevated temperatures up to 100 °C, both E_c and the remanent polarization P_{rem} reduce considerably. The "pinching" of the polarization loop at elevated temperatures indicates a change to the polarization reversal mechanism.

Figure 1(b) shows the strain hysteresis loops measured simultaneously with the polarization. Similar behavior in terms of maximum strain and E_c is observed with increasing temperature. The reduced remanent strain leads to a distinct

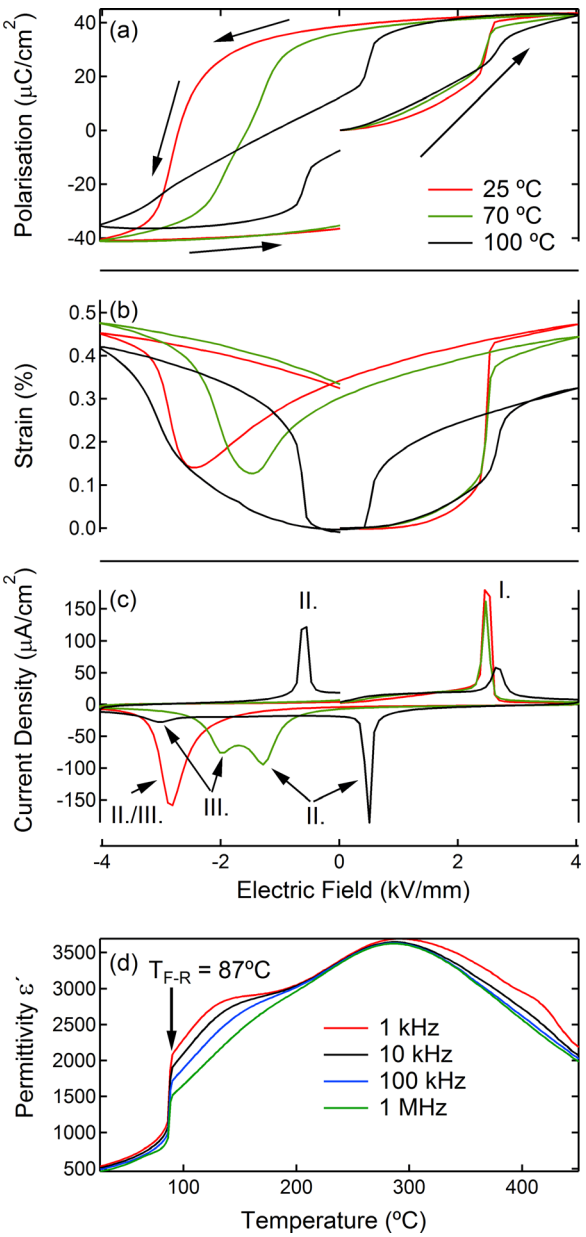

FIG. 1. (a) Polarization, (b) strain, and (c) current density hysteresis loops upon first application of a bipolar electric field starting with positive polarity (indicated by the arrows in (a)) and measured at three different temperatures as well as (d) temperature dependent permittivity measured on an electrically poled sample upon heating at four different frequencies.

change in the shape of the strain hysteresis loop and a continuous increase of the unipolar strain up to about 0.3% at 100 °C.

Figure 1(c) depicts the current density corresponding to the bipolar polarization measurement in Figure 1(a). During the positive half-cycle, the current density increases slightly with electric field amplitude up to ~2 kV/mm. Beyond this, a sharp peak (labeled with "I.") occurs that corresponds to the strong increase in polarization and strain upon poling.

The average crystallographic structure of unpoled ceramics with compositions close to BNT-6BT is reportedly pseudo-cubic with no long-range polar order. However, polar regions with presumably antiferroelectric ordering may exist on the local scale embedded in the non-polar matrix.[12] Upon electrical poling, a long-range order and strong crystallographic texture is established if a sufficiently high electric

field is applied.[5,25] This simultaneous structural phase transition and domain texturing give rise to the poling peak in the current density hysteresis observed in the first positive half-cycle in Fig. 1(c). The electric field at which peak I. occurs shifts only slightly with increasing temperature, whereas its amplitude decreases.

The polarization reversal process is revealed during the negative half cycle of the current density loops. At room temperature, only one, broad current density peak is observed at −2.8 kV/mm (labelled "II./III."), in a manner resembling soft lead-zirconate-titanate (PZT).[26] As the temperature is increased to 50 °C, this current density peak occurs at progressively lower electric field magnitudes, suggesting energetically easier polarization reversal. Between 50 °C and 70 °C, the single peak starts to split in two (labelled "II." and "III."). While peak II. continues to move to lower electric field offsets, peak III. shifts to higher fields, reflecting the onset of the "pinching" of the polarization hysteresis (Fig. 1(a)). The characteristics of these two current density peaks have different temperature dependences. The high-field peak III. maintains a broad shape albeit with diminished current amplitude and shifts to higher fields with increased temperature. In contrast, the low-field peak II. sharpens and shifts to lower fields with increased temperature. For the highest temperature of 100 °C, peak II. crosses the 0 kV/mm offset field, occurring under a positive electric field polarity.

The results indicate that with increasing temperature the polarization reversal mechanism changes from a one-step to a two-step process. For ferroelectric ceramics, the polarization reversal process occurs over a broad distribution of local electric fields.[27,28] This is evidenced in our results by the broad single current density peak II./III. observed close to room temperature. Comparing the evolution of the polarization and strain responses upon electric field reversal, it becomes clear that the emergence of peak II. in the current density upon increased temperature is associated with the loss of remanent polarization and strain, i.e., a de-poling process. "Pinching" of the polarization loop can originate from different mechanisms: (1) time dependent aging,[29] (2) a reversible phase transformation between an antiferroelectric and a ferroelectric phase affecting the whole sample,[30] and (3) the decay of a long-range ordered ferroelectric state into a short-range ordered relaxor state.[17] Aging as origin of the observed pinching feature can be ruled out immediately, as no time dependent changes to the hysteresis loops have been observed.

In-situ synchrotron diffraction experiments clarify the structural dynamics of the temperature dependent polarization reversal process. The electric field dependent profiles of the (111) and (200) reflections parallel to the electric field direction are shown in Figure 2 for 25 °C (a), 70 °C (b) and 100 °C (c). At all temperatures, the profiles of both reflections prior to field application are single peaks consistent with the expected non-polar, pseudo-cubic average structure.

At 25 °C, the strongest structural changes occurred upon the initial field application. At low field amplitudes, the profiles shift to lower 2θ. At a critical threshold field, the (200) reflection then splits into two components. This response is captured in the macroscopic data by the sharp current density peak I. in the first positive half-cycle. Upon electric field reversal, the (111) reflection broadens, while the induced low-angle peak in the (200) reflections progressively reduces in intensity as the field reaches its minima. The remaining high angle peak of the (200) reflections increases in intensity continuously over the same period. Only minor changes to the profile position and intensity are observed with further cycling. These observations are consistent with an initial pseudo-cubic to tetragonal transformation, however, on polarization reversal and subsequent cycling, the sample appears to be mixed phase rhombohedral and tetragonal.[6,31,32] Detailed scans of the (111) and (200) reflections in the virgin state and during high field application are given in supplementary Figure S1.[33]

At 70 °C, the initial field-induced transformation results in a lowering of the intensity, increases in width, and shifts in both the (111) and (200) peaks. This behavior is consistent with an induced mixed tetragonal and rhombohedral symmetry with strong domain texturing. The broad, low-intensity profiles associated with the field-induced structure remain

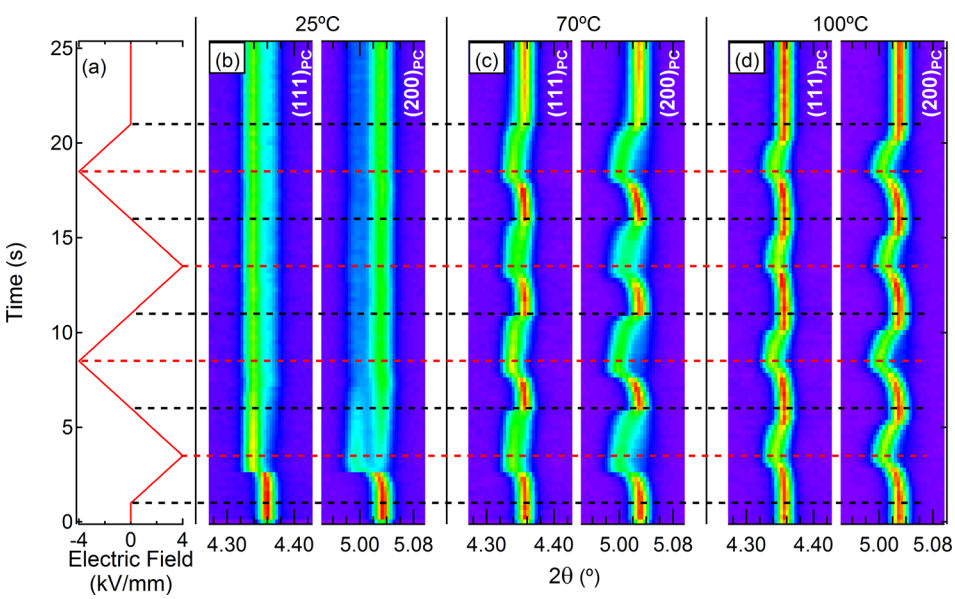

FIG. 2. *In-situ* diffraction measurements taken during application of a bipolar electric field, (a) schematic of the applied electric field signal over time, (111) and (200) reflections recorded at (a) 25 °C, (b) 70 °C, and (c) 100 °C.

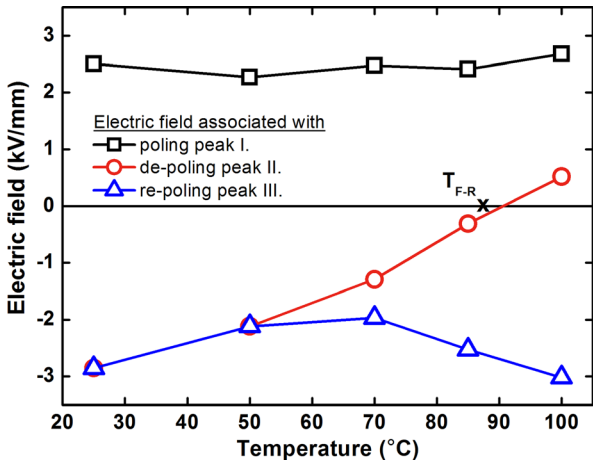

FIG. 3. Electric field-temperature (E-T) diagram showing the electric field corresponding to the peak positions of the current density for several temperatures. $T_{F\text{-}R} = 87\,^{\circ}C$ as determined from a temperature dependent permittivity measurement is marked with "X."

until the electric field is reversed. At small negative fields, the structure briefly returns to the initial pseudo-cubic state (i.e., non-polar average structure) before being re-transformed into the strongly textured mixed phase polar structure. This process appears to be reversible and is correlated to the onset of the peak splitting in the current density and the pinching of the polarization hysteresis around 70 °C.

Similar features have been observed for an antiferroelectric ceramic and were related to an electric field induced transition from a ferroelectric to an antiferroelectric state triggered by the volume contraction occurring at the application of the coercive field with reverse polarity.[34] However, the association of the polarization hysteresis pinching with the transformation between a polar average structure and a non-polar average structure highlights that the underlying mechanism is not based on a ferroelectric-antiferroelectric transformation (which is a transformation that involves splitting of the diffraction peaks due to distortions from the average cubic structure), but rather related to the relaxor characteristics of the material.

At 100 °C, the stability of the induced polar phases reduces further (Figure 2(d)). The electric field range where the (111) and (200) reflection profiles show broadening characteristics of an induced mixed-phase structure shrinks considerably, and the degradation into the non-polar state occurs before the field magnitude reaches 0 kV/mm for both the positive and negative half-cycles. This is consistent with the loss of remanent polarization and strain, and the emergence of a current density peak upon reduction of the electric field strength but before the field polarity is reversed.

In Figure 3, the temperature dependent electric field values associated with the three current density peaks (Fig. 1(c)) are summarized in an electric field-temperature (E-T) diagram.[15] The transition temperature $T_{F\text{-}R}$ determined from temperature dependent permittivity measurements is marked for reference. The diagram shows that the temperature at which the ferroelectric-to-relaxor decay occurs spontaneously (i.e., the electric field associated with the de-poling peak II. switches from negative to positive polarity) is similar to $T_{F\text{-}R}$ extracted from the permittivity measurements. This is expected as the permittivity measurement was conducted without the application of a large offset field and reflects the pure temperature dependent behavior. However, the temperature at which the current density peaks start to split is found to be about 25 °C lower than $T_{F\text{-}R}$, highlighting the impact of an electric bias field on the characteristics of the ferroelectric-to-relaxor transition.

It is important to note that the processes probed by polarization and current density measurements occur on a macroscopic scale and do not allow quantitative conclusions about structural changes. In contrast, the temperature $T_{F\text{-}R}$ extracted from temperature dependent permittivity measurements is associated with the transition from a polar long-range order to a non-polar relaxor structure and is thus correlated to structural change. The depolarization temperature T_d at which the ferroelectric polarization vanishes is usually found to be just slightly lower than $T_{F\text{-}R}$,[18] indicating a close relation between macroscopic depolarization and transition into the relaxor state. However, in the current study, the observed difference between $T_{F\text{-}R}$ and the temperature related to the appearance of the double peaks in the current density (Figure 1(c)) suggests that the depolarization process can be triggered by an electric field of reverse polarity already at temperatures well below the structural transition temperature $T_{F\text{-}R}$.

It is reported that the polarization reversal process in lead-based relaxors can be described as a transition from one long-range order state to another upon electric field reversal, occurring through a nano-domain state without long-range order triggered by low electric fields. The occurrence of depolarization fields developing at the phase boundaries has been suggested as a trigger for "backswitching" into the nano-domain state.[35] Most interestingly, this phenomenon was also found to exist well below the transition temperature $T_{F\text{-}R}$.[36]

The temperature independence of the poling peak I. hints at the transitional changes occurring in the polarization reversal process upon temperature increase. The critical electric field required to trigger the transformation from the relaxor into the ferroelectric state appears to be only slightly dependent on temperature (Figure 3). If we assume that the entire sample is transformed into a relaxor-like state upon electric field reversal, we would expect to see the same temperature independent behavior of the re-poling peak position (peak III.). Instead, a continuous shift to higher electric fields with increasing temperature is observed, reaching similar absolute values to the electric field amplitude associated with poling peak I. for temperatures above 85 °C. This behavior, as observed in the medium temperature regime (~50–80 °C), can be rationalized as a combination of both (1) a conventional ferroelectric domain reversal processes that may involve a combination of 180° and non-180° switching steps and (2) polarization reversal through an intermediate relaxor phase. For temperatures higher than $T_{F\text{-}R}$, the reversal mechanism becomes dominated by the phase transformation-based process. The de-polarization behavior and as such the ferroelectric-to-relaxor transformation appear to be strongly dependent on both temperature and electric field, making it a kinetically controlled process that presumably shows strong dispersive behavior. In the present study,

both phase transformation and domain switching processes related to the depolarization occur simultaneously such that the kinetics of each process cannot be resolved explicitly. It is known that polarization switching is a rather slow process.[28] In contrast, the abrupt changes in current density and crystallographic structure observed in the present study indicate that the phase transition into the relaxor state occurs quite rapid suggesting faster kinetics compared to the domain switching mechanism. This speculation is supported by the finding that the phase transformation in BNT-based relaxor materials gets suppressed if the frequency of the applied electric field is too low,[37] indicating vice versa that the phase transformation can still occur at higher frequencies for which domain switching already gets delayed.

In contrast, the poling process starting from a pure relaxor phase lacks this kind of dependency in the observed temperature range and occurs as soon as a threshold field is exceeded. This conclusion is further supported by the diffraction data, where the electric field at which the initial structural change (i.e., the splitting of the (200) reflection) occurs remains approximately constant across the measured temperature range.

The mechanism of polarization reversal depends significantly on the stability of the electric-field-induced ferroelectric phase. At low temperatures, the polarization reversal process is governed by ferroelectric domain switching. With increasing temperature, the ferroelectric phase destabilizes and polarization reversal starts to occur through a double phase transition through a non-polar relaxor state. The decay into the relaxor state is not an instantaneous process but occurs already at temperatures approximately 25 °C lower than $T_{F\text{-}R}$. Below $T_{F\text{-}R}$, small electric fields of reverse polarity are needed to trigger the transition into the non-polar relaxor state, which might be associated to the presence of depolarization fields reducing the stability of the ferroelectric phase. Even though the commonly reported $T_{F\text{-}R}$ and T_d, as extracted from small signal permittivity and piezoelectric coefficient measurements, give a good indication of the working temperature regime of a certain composition, the dynamics of the depolarization process makes it necessary to create E-T diagrams from large signal measurements to identify the best temperature regimes for actuator applications.

We are grateful to the European Synchrotron Radiation Facility for the provision of experimental beamtime. This work was supported through the Australian Research Council Project Nos. DE120102644 and DP120103968. H.S. acknowledges support from an individual postdoctoral grant from the Danish Council of Independent Research, DFF-FTP.

[1]J. Rödel, W. Jo, K. T. P. Seifert, E.-M. Anton, T. Granzow, and D. Damjanovic, J. Am. Ceram. Soc. **92**, 1153 (2009).
[2]D. Schütz, M. Deluca, W. Krauss, A. Feteira, T. Jackson, and K. Reichmann, Adv. Funct. Mater. **22**, 2285 (2012).
[3]P. M. Gehring, J. Adv. Dielectr. **02**, 1241005 (2012).
[4]A. A. Bokov and Z.-G. Ye, J. Mater. Sci. **41**, 31 (2006).
[5]J. E. Daniels, W. Jo, J. Rödel, and J. L. Jones, Appl. Phys. Lett. **95**, 32904 (2009).
[6]H. Simons, J. Daniels, W. Jo, R. Dittmer, A. Studer, M. Avdeev, J. Rödel, and M. Hoffman, Appl. Phys. Lett. **98**, 082901 (2011).
[7]S.-T. Zhang, A. B. Kounga, E. Aulbach, T. Granzow, W. Jo, H.-J. Kleebe, and J. Rödel, J. Appl. Phys. **103**, 034107 (2008).
[8]E. A. Patterson and D. P. Cann, J. Am. Ceram. Soc. **95**, 3509 (2012).
[9]J. Glaum, H. Simons, M. Acosta, and M. Hoffman, J. Am. Ceram. Soc. **96**, 2881 (2013).
[10]W. Jo, S. Schaab, E. Sapper, L. A. Schmitt, H.-J. Kleebe, A. J. Bell, and J. Rödel, J. Appl. Phys. **110**, 074106 (2011).
[11]G. Burns and F. H. Dacol, Phys. Rev. B **28**, 2527 (1983).
[12]C. Ma, X. Tan, E. Dul'kin, and M. Roth, J. Appl. Phys. **108**, 104105 (2010).
[13]X. Tan, C. Ma, J. Frederick, S. Beckman, and K. G. Webber, J. Am. Ceram. Soc. **94**, 4091 (2011).
[14]A. A. Bokov and Z. Ye, Solid State Commun. **116**, 105 (2000).
[15]V. Bobnar, Z. Kutnjak, R. Pirc, and A. Levstik, Phys. Rev. B **60**, 6420 (1999).
[16]Z.-G. Ye and H. Schmid, Ferroelectrics **145**, 83 (1993).
[17]W. Jo, R. Dittmer, M. Acosta, J. Zang, C. Groh, E. Sapper, K. Wang, and J. Rödel, J. Electroceram. **29**, 71 (2012).
[18]E. Sapper, S. Schaab, W. Jo, T. Granzow, and J. Rödel, J. Appl. Phys. **111**, 014105 (2012).
[19]W. Jo, J. Daniels, D. Damjanovic, W. Kleemann, and J. Rödel, Appl. Phys. Lett. **102**, 192903 (2013).
[20]S.-T. Zhang, A. B. Kounga, E. Aulbach, W. Jo, T. Granzow, H. Ehrenberg, and J. Rödel, J. Appl. Phys. **103**, 034108 (2008).
[21]M. Acosta, J. Zang, W. Jo, and J. Rödel, J. Eur. Ceram. Soc. **32**, 4327 (2012).
[22]J. E. Daniels and M. Drakopoulos, J. Synchrotron Radiat. **16**, 463 (2009).
[23]J. E. Daniels, A. Pramanick, and J. L. Jones, IEEE Trans. Ultrason., Ferroelectr., Freq. Control **56**, 1539 (2009).
[24]J. E. Daniels, W. Jo, J. Rödel, V. Honkimäki, and J. L. Jones, Acta Mater. **58**, 2103 (2010).
[25]C. Ma, H. Guo, S. P. Beckman, and X. Tan, Phys. Rev. Lett. **109**, 107602 (2012).
[26]K. B. Chong, F. Guiu, and M. J. Reece, J. Appl. Phys. **103**, 014101 (2008).
[27]S. Zhukov, Y. A. Genenko, and H. von Seggern, J. Appl. Phys. **108**, 014106 (2010).
[28]Y. A. Genenko, S. Zhukov, S. V. Yampolskii, J. Schütrumpf, R. Dittmer, W. Jo, H. Kungl, M. J. Hoffmann, and H. von Seggern, Adv. Funct. Mater. **22**, 2058 (2012).
[29]Y. A. Genenko, J. Glaum, M. J. Hoffmann, and K. Albe, Mater. Sci. Eng., B **192**, 52 (2015).
[30]W.-H. Chan, H. Chen, and E. V. Colla, Appl. Phys. Lett. **82**, 2314 (2003).
[31]H. Simons, J. Glaum, J. E. Daniels, A. J. Studer, A. Liess, J. Rödel, and M. Hoffman, J. Appl. Phys. **112**, 044101 (2012).
[32]W. Jo, J. E. Daniels, J. L. Jones, X. Tan, P. A. Thomas, D. Damjanovic, and J. Rödel, J. Appl. Phys. **109**, 014110 (2011).
[33]See supplementary material at http://dx.doi.org/10.1063/1.4937586 for diffraction peak profiles around the pseudo-cubic (111) and (200) in the initial and first high field states for (a) 70 °C and (b) 100 °C.
[34]X. Tan, J. Frederick, C. Ma, W. Jo, and J. Rödel, Phys. Rev. Lett. **105**, 255702 (2010).
[35]V. Y. Shur, E. L. Rumyantsev, G. G. Lomakin, O. V. Yakutova, D. V. Pelegov, A. Sternberg, and M. Kosec, Ferroelectrics **314**, 245 (2005).
[36]S. Schaab and T. Granzow, Appl. Phys. Lett. **97**, 132902 (2010).
[37]A. J. Royles, A. J. Bell, J. E. Daniels, S. J. Milne, and T. P. Comyn, Appl. Phys. Lett. **98**, 182904 (2011).